






RESEARCH ARTICLE

Plasma lipid metabolites associate with diabetic polyneuropathy in a cohort with type 2 diabetes

Amy E. Rumora^{1,2,*} , Kai Guo^{2,3,*}, Fadhl M. Alakwaa^{1,2}, Signe T. Andersen⁴, Evan L. Reynolds^{1,2} , Marit E. Jørgensen^{5,6}, Daniel R. Witte^{4,7}, Hatice Tankisi⁸ , Morten Charles⁴, Masha G. Savelieff², Brian C. Callaghan^{1,2} , Troels S. Jensen⁹ & Eva L. Feldman^{1,2} 

¹Department of Neurology, University of Michigan, Ann Arbor, Michigan

²NeuroNetwork for Emerging Therapies, University of Michigan, Ann Arbor, Michigan

³Department of Biomedical Sciences, University of North Dakota, Grand Forks, North Dakota

⁴Department of Public Health, Aarhus University, Aarhus, Denmark

⁵Steno Diabetes Center Copenhagen, Gentofte, Denmark

⁶University of Southern Denmark, Odense, Denmark

⁷Danish Diabetes Academy, Odense, Denmark

⁸Department of Clinical Neurophysiology, Aarhus University, Aarhus, Denmark

⁹Danish Pain Research Center, Department of Clinical Medicine, Aarhus University, Aarhus, Denmark

Correspondence

Eva L. Feldman, Russell N. DeJong Professor of Neurology, 5017 AAT-BSRB, 109 Zina Pitcher Place, Ann Arbor, MI 48109.
Tel: +1 (734) 763-7274; Fax: +1 (734) 763-7275;
E-mail: efeldman@umich.edu

Funding Information

This work was supported by the Novo Nordisk Foundation through a Novo Nordisk Foundation Challenge Programme grant [grant number NNF14OC0011633]; the National Institutes of Health [grant numbers 1R24DK082841, 1R21NS102924, 1DP3DK094292, 1F32DK112642, 1K99DK119366, and T32NS0007222]; the American Diabetes Association [grant number 7-12-BS-045]; the NeuroNetwork for Emerging Therapies; and the A. Alfred Taubman Medical Research Institute.

Received: 23 December 2020; Revised: 30 March 2021; Accepted: 31 March 2021

Annals of Clinical and Translational Neurology 2021; 8(6): 1292–1307

doi: 10.1002/acn3.51367

*Amy E. Rumora and Kai Guo contributed equally to this study.

Introduction

Diabetic polyneuropathy (DPN) is the most prevalent diabetes complication, affecting up to 50% of individuals

Abstract

Objective: The global rise in type 2 diabetes is associated with a concomitant increase in diabetic complications. Diabetic polyneuropathy is the most frequent type 2 diabetes complication and is associated with poor outcomes. The metabolic syndrome has emerged as a major risk factor for diabetic polyneuropathy; however, the metabolites associated with the metabolic syndrome that correlate with diabetic polyneuropathy are unknown. **Methods:** We conducted a global metabolomics analysis on plasma samples from a subcohort of participants from the Danish arm of Anglo-Danish-Dutch study of Intensive Treatment of Diabetes in Primary Care (ADDITION-Denmark) with and without diabetic polyneuropathy versus lean control participants. **Results:** Compared to lean controls, type 2 diabetes participants had significantly higher HbA1c ($p = 0.0028$), BMI ($p = 0.0004$), and waist circumference ($p = 0.0001$), but lower total cholesterol ($p = 0.0001$). Out of 991 total metabolites, we identified 15 plasma metabolites that differed in type 2 diabetes participants by diabetic polyneuropathy status, including metabolites belonging to energy, lipid, and xenobiotic pathways, among others. Additionally, these metabolites correlated with alterations in plasma lipid metabolites in type 2 diabetes participants based on neuropathy status. Further evaluating all plasma lipid metabolites identified a shift in abundance, chain length, and saturation of free fatty acids in type 2 diabetes participants. Importantly, the presence of diabetic polyneuropathy impacted the abundance of plasma complex lipids, including acylcarnitines and sphingolipids. **Interpretation:** Our explorative study suggests that diabetic polyneuropathy in type 2 diabetes is associated with novel alterations in plasma metabolites related to lipid metabolism.

with diabetes worldwide.¹ DPN is characterized by progressive, length-dependent nerve damage, which causes pain or sensory loss in the limbs and results in severe morbidity, falls, amputations, and a lower quality of life.¹

Hyperglycemia is a major DPN risk factor in type 1 diabetes (T1D), where tight glycemic control effectively slows DPN progression.² However, glycemic control does not effectively slow DPN progression in type 2 diabetes (T2D),³ suggesting that additional risk factors are involved.⁴ These studies highlight that the metabolic factors underlying DPN progression are distinct in T2D versus T1D.⁴

In patient cohorts, we have shown that the metabolic syndrome (MetS) is a major independent DPN risk factor in T2D.^{3,5} MetS is highly prevalent in T2D populations^{3,5} and is defined by five metabolic components, including obesity and dyslipidemia, which are characterized by low high-density lipoproteins (HDLs) and hypertriglyceridemia.⁶ In the Danish arm of the Anglo-Danish-Dutch study of Intensive Treatment of Diabetes in Primary Care (ADDITION), we identified waist circumference and low plasma HDL cholesterol, a MetS dyslipidemia component, as T2D DPN risk factors.⁷ Alongside these MetS components, elevated levels of methylglyoxal, an oxidative stress biomarker, also correlated with T2D DPN in ADDITION-Denmark, indicative of broader plasma metabolic changes. Importantly, we most recently concluded from an ADDITION-Denmark analysis that lipid-lowering statins do not alter DPN incidence, suggesting that hyperlipidemia per se may not cause DPN, but rather that changes in specific lipids or metabolites may underlie DPN.⁸ However, the specific metabolite and lipid species associated with MetS in T2D DPN progression are not fully understood.

In this study, we identified alterations in circulating metabolites and lipids that correlate with T2D DPN by conducting global metabolomics analysis on plasma from healthy individuals and from T2D and T2D DPN participants enrolled in ADDITION-Denmark.^{7,9} We identified 15 metabolites that differed in T2D DPN versus T2D participants, which included complex lipids. These data support the idea that prevalent DPN in T2D correlates with a specific plasma metabolite and lipid profile.

Methods

Study population

This cross-sectional case-control study included participants with screen-detected T2D with or without DPN and healthy controls. The diabetes cohort is a subpopulation of participants that attended a clinical follow-up examination between October 2015 and June 2016 at the Aarhus study site of ADDITION-Denmark. Briefly, ADDITION-Denmark enrolled participants (40–69 year of age) with previously undiagnosed, screen-detected T2D between 2001 and 2006. During the trial, which ended in

2009, general practices were randomly assigned to provide T2D participants with routine care or a more intensive multifactorial treatment.¹⁰ After a mean of 13 years post-enrollment in ADDITION-Denmark, the T2D cohort ($N = 97$) in the current study underwent follow-up examination.⁹ Participants fasted from midnight the previous day until their examination, which involved blood sample collection, vitals, anthropometric measurements, and DPN assessment, which were all conducted on the same visit. Out of 97 participants, 48 were identified with DPN and 49 without DPN. The age- and sex-matched healthy control participants without T2D ($N = 9$) were from the same geographical area and were derived from the original ADDITION-Denmark screen. At examination, healthy control participants were evaluated to confirm that they had not developed diabetes or another neurological disease and had normal nerve conduction studies (NCS).

DPN assessment

DPN was assessed by NCS, as defined by published criteria,¹¹ using Keypoint. Net EMG equipment (Dantec, Skovlunde, Denmark). The Z-scores of in-house age- and height-matched normative data were used to calculate sum scores from the average of the following six parameters: peroneal, tibial, and median nerve NCVs, tibial and median nerve minimum F-wave latencies, and sural sensory nerve action potential amplitude. The ulnar nerve was assessed instead of the median nerve when NCS indicated the presence of carpal tunnel syndrome. NCS sum Z-scores >2.0 were considered abnormal and indicated DPN.

Vitals, basic metabolic profile, and anthropometric measurements

Each participant received a clinical examination, which included vitals (systolic and diastolic blood pressure), anthropometric measurements (weight, height, BMI, waist circumference), and metabolic measures from blood [total cholesterol, HDL cholesterol, triglycerides, glycated hemoglobin (HbA1c)] and urine (creatinine) samples. Age, sex, and prescribed medication (glucose-lowering drugs, statins, β -blockers, antihypertensives, and aspirin) were also collected.

Metabolomic profiling

Plasma samples from each participant were shipped on dry ice to Metabolon (Durham, NC), and stored at -80°C for metabolomics profiling. For analysis, recovery and internal standards were added to each plasma sample

to evaluate extraction and instrument variability, respectively. Methanol was added to precipitate protein and dissociate protein-bound metabolites and extract chemically diverse metabolites from solution. After centrifugation, the supernatant was aliquoted into several portions, for analysis by three different types of ultra-performance liquid chromatography tandem mass spectroscopy (UPLC-MS/MS). The methanol was evaporated from the supernatant aliquot and the dry metabolite residue was reconstituted in solvents appropriate for each of the following: reverse phase UPLC-MS/MS in positive and negative ion mode electrospray ionization (ESI) and hydrophilic interaction liquid chromatography UPLC-MS/MS in negative ion mode ESI. This approach analyzes nonpolar and polar metabolites and lipids. A detailed description of Metabolon's protocols for sample preparation, quality assurance, quality control, and data normalization are described in File S1.

Metabolite identification and quantification

Metabolite peaks were quantified by calculating the area under the curve. Day-to-day run variation for each metabolite was corrected daily by equaling the median to 1.00 to normalize each metabolite data point by sample. In total, 991 metabolites were identified by automated comparison of ion features from each sample to a reference library of chemical standards of known specific retention times/indexes and mass-to-charge ratios.

Metabolomics data processing

Metabolites below the detection limit (missed in over 50% of all samples) were removed from further analysis. The remaining metabolites had less than 50% missingness and missing values were imputed using the K-Nearest Neighbors (KNN) algorithm.¹² The 50% threshold is the default threshold in the Metaboanalyst R package. Data were log transformed to reduce heteroscedasticity of metabolite values. A principal component analysis (PCA) plot was used to detect outliers and visualize participant group separation.¹³

Statistics

Statistical analysis

Descriptive statistics were used to compare demographic and metabolic information across participant groups (Controls, T2D, T2D DPN). Fisher's Exact Tests were used to compare the distribution of sex between participant groups (Control vs. T2D and T2D vs. T2D DPN), and a Wilcoxon signed rank test was used to compare

diabetes duration between T2D participants with and without DPN. In addition, one-way ANOVA with Tukey's honest significant difference tests were used to make pairwise comparisons of age and continuous metabolic factors between participant groups (Control vs. T2D and T2D vs. T2D DPN).

Univariate analysis

Independent two-sample *t*-tests were used to assess the unadjusted pairwise differences in each metabolite between participant groups (Control vs. T2D, Control vs. T2D DPN, and T2D vs. T2D DPN). In addition, linear regression models were used to identify metabolites that significantly differed between participant groups, after adjusting for participant age, sex, and medication use. Given a large number of comparisons, to control the false discovery rate, we also calculated *Q*-values for the unadjusted comparisons.^{14,15} Boxplots were used to visualize the distribution of *Q*-values and *p*-values corresponding to the unadjusted and adjusted pairwise comparisons. Boxplots were also used to display the abundance of metabolites that were significantly different across participant groups.

Feature selection and ranking

A penalized logistic regression method, "elastic net," from glmnet R package¹⁶ was used to select metabolites that segregated T2D from T2D DPN participants. We performed 10-fold cross-validation by tuning two penalty parameters, alpha and lambda. Alpha sets the mixing degree between ridge regression (alpha = 0) and lasso (alpha = 1), whereas lambda controls the shrink rate of metabolite coefficients. Partial least squares discriminant analysis (PLS-DA) was used to measure the importance score of the metabolites selected by an elastic net.¹³ The importance score indicates the contribution of each metabolite to the model.

Classification and feature importance

Lilikoil R package¹⁷ and elastic net-selected metabolites were used to build different classifiers using seven machine learning algorithms, including Linear Discriminant Analysis, Support Vector Machine, Random Forest (RF), Recursive Partitioning and Regression Trees, Prediction Analysis for Microarrays, Logistic Regression, and Gradient Boosting Machine (GBM). Classification And Regression Training (CARET) R package¹⁸ was used to perform cross-validation, features ranking, and training-testing split. A 10-fold setting on the training dataset was used to avoid overfitting. Prediction accuracy metrics

included area under the receiver operating characteristic curve (AUC), sensitivity, and specificity. The pROC R package¹⁹ was employed to plot receiver operating characteristic curves. The VarImp function from CARET was implemented to rank metabolites based on their contribution to model performance.

Correlation analysis

Based on the association between DPN and MetS,³ Spearman's rank correlation coefficients were computed between the top eight elastic net metabolites to all lipids. Heat maps were generated to plot the Spearman's correlation coefficients. Heat maps were also used to display differences in free fatty acid and complex lipid abundance. A *t*-test was used to identify significantly altered lipids in T2D DPN compared to T2D.

Data and resource availability

The data collected from this study have been deposited to the metabolomics workbench repository (<https://www.metabolomicsworkbench.org/>, study ID ST001411).

Ethics

The study was approved by the Committee on Health Research Ethics in the Central Denmark Region (file nos. 20000183 and 1-10-72-63-15) and the Danish Data Protection Agency (file no. 2005-57-0002, ID185). The study was conducted in accordance with the principles of the Declaration of Helsinki, version 1996, and all study participants gave written informed consent.

Results

Cohort characteristics

Cohort characteristics are presented in Table 1.⁷ Participants did not differ significantly by age, sex, blood pressure, or urine creatine. As anticipated, HbA1c was elevated in T2D versus healthy participants, and, although fasting blood glucose was not recorded at the 13-year follow-up appointment, we detected a distinct increase in the glucose metabolite in T2D versus lean participants in the metabolomics data (metabolite #1071, Table S1). BMI and waist circumference were also higher in T2D participants compared to controls, which we expect since obesity is a frequent T2D comorbidity.^{7,20} T2D participants had significantly lower total cholesterol than healthy participants; however, there was also a trending increase in triglycerides and decrease in HDL, which did not attain significance. The more favorable total cholesterol profile

in the T2D cohort may be due to prevalent statin use (Fig. 1A), whereas β -blockers may have contributed to the trending increase in triglycerides (Fig. 1B).²¹ Importantly, there were no significant differences in any metric between T2D participants with or without DPN, although there were trending increases in HbA1c, diabetes duration, and triglycerides. Although baseline or uncontrolled hyperglycemia² and dyslipidemia²⁰ are T2D DPN risk factors, controlling these metabolic parameters does not necessarily prevent DPN onset and progression. Thus, we next sought to identify specific differential metabolites and lipids in T2D participants with and without DPN by global metabolomics.

Bioinformatics pipeline

Our bioinformatics pipeline is outlined in Figure 2. First, untargeted global metabolomics identified 991 total metabolites. Approximately 75 metabolites (7%) were below the detection limit and removed from further analysis (Table S2), leaving 916 metabolites. Missing metabolite values were imputed by KNN and a PCA plot was used to visualize the results. Second, linear regression and elastic net models identified significantly differentiated metabolites in T2D versus T2D DPN. PLS-DA of elastic net metabolites was used to generate metabolite importance scores. We also built classifiers using different machine learning algorithms. Third, we assessed the predictability of the metabolites by power analysis and calculated the correlation between elastic net metabolites to lipids metabolites.

Plasma metabolomics reveals metabolites that differentiate T2D participants by DPN status

PCA revealed distinct metabolite profiles between T2D and control participants, however, there was no clear separation between T2D participants with and without DPN (Fig. 3A). Unadjusted results from the independent two-sample *t*-tests revealed there were 254 metabolites that were significantly different between T2D and control participants, and 28 that were significantly different between T2D participants with and without DPN ($p < 0.05$) (Table S1). *Q*-values for unadjusted comparison of the 254 metabolites showed that 92 metabolites that were significantly different between lean controls and T2D participants, and 28 metabolites that were significantly different between T2D participants with and without DPN, could possibly be false discoveries (Fig. 3B and Table S1). After adjusting for age, sex, and medication use, there were 124 metabolites that differed between all T2D versus control participants and 18 that differed between T2D

Table 1. Participant demographics at the time of plasma collection for global metabolomics analysis in a subcohort of ADDITION-Denmark.

Parameter	Control (N = 9)	T2D (N = 49)	T2D DPN (N = 48)	p-value
Age, mean (SD), years	71.38 ± 4.34	71.28 ± 6.16	71.05 ± 6.05	*p = 0.999 #p = 0.9794
Sex				*p = 0.6683 #p = >0.9999
Female	1 (11.11%)	11 (22.45%)	11 (22.92%)	
Male	8 (88.89%)	38 (77.55%)	37 (77.08%)	
Diabetes duration, mean (SD), years	N/A	11.76 ± 1.94	12.11 ± 1.98	#p = 0.8489
HbA1c, mean (SD)	36.33 ± 3.00	49.92 ± 9.08	54.29 ± 13.47	*p = 0.0028 #p = 0.1301
BMI, mean (SD), kg/m ²	23.89 ± 2.26	31.31 ± 4.93	31.15 ± 5.64	*p = 0.0004 #p = 0.9794
Weight, mean (SD), kg	73.17 ± 10.17	91.58 ± 14.98	94.44 ± 19.40	*p = 0.0091 #p = 0.6817
Waist, mean (SD), cm	89.11 ± 8.15	107.61 ± 10.24	109.25 ± 13.86	*p = 0.0001 #p = 0.7786
Blood pressure, mean (SD), mm Hg				
Systolic	137.56 ± 15.73	138.98 ± 15.13	141.33 ± 17.96	*p = 0.9694 #p = 0.7632
Diastolic	82.89 ± 8.74	82.76 ± 10.68	82.92 ± 8.36	*p = 0.9992 #p = 0.9962
Total cholesterol, mean (SD), mmol/L	6.06 ± 1.93	4.47 ± 0.83	4.26 ± 0.96	*p = 0.0001 #p = 0.5817
Triglycerides, mean (SD), mmol/L	1.12 ± 0.44	1.69 ± 0.74	1.93 ± 1.18	*p = 0.2260 #p = 0.4312
HDL Cholesterol, mean (SD), mmol/L	1.78 ± 0.42	1.47 ± 0.46	1.39 ± 0.36	*p = 0.1067 #p = 0.5840
Creatine, mean (SD), mmol/L	87.44 ± 19.45	83.69 ± 18.68	79.09 ± 17.89	*p = 0.8400 #p = 0.4368

BMI, body mass index; DPN, diabetic polyneuropathy; HbA1c, hemoglobin A1c; HDL, high-density lipoprotein; N/A, not applicable; SD, standard deviation; T2D, type 2 diabetes.

*Control versus T2D; #T2D versus T2D DPN; significantly different parameters are in bold.

Participant sex p-value was assessed using a Fishers Exact Test. Diabetes duration p-value was assessed using a Wilcoxon matched-pairs signed rank test. For all other parameters, p-value was determined by using an Ordinary one-way ANOVA with Tukey's Multiple Comparisons.

participants with and without DPN, of which 12 metabolites were unique ($p < 0.05$) (Fig. 3C). Boxplots summarizing the distribution of p-values and Q-values corresponding to the adjusted and unadjusted participant group comparisons are presented in Figure S1. The 12 metabolites that were different between control, T2D, and T2D DPN participant groups are involved in lipid metabolism [isoursodeoxycholate sulfate, glycosyl-N-(2-hydroxynervonoyl)-sphingosine (d18:1/24:1(2OH)), 3-carboxy-4-methyl-5-propyl-2-furanpropanoate (CMPF)], amino acids (4-methyl-2-oxopentanoate, N-acetyl-3-methylhistidine), and energy (citrate) (Fig. 3D). We also identified metabolites related to carbohydrates (arabinose) and xenobiotics (tartrate, 3,5-dichloro-2,6-dihydroxybenzoic acid, 3-bromo-5-chloro-2,6-dihydroxybenzoic acid, 3-formylindole, sulfate of piperine).

To adjust for collinearity, we used elastic net, a regularized logistic regression method, which identified eight significantly differential metabolites in T2D versus T2D

DPN participants. These were categorized as lipids [isoursodeoxycholate sulfate, ximenoylcarnitine (C26:1)], energy (citrate), amino acids (N-acetyl-3-methylhistidine, N-acetyl-β-alanine), and xenobiotics [tartrate, perfluorooctanoate (PFOA), sulfate of piperine]. A heat map demonstrates distinct differences in the abundance of these eight metabolites in T2D participants with and without DPN (Fig. 4A). Analysis of their mean relative abundances indicated five were downregulated and three were upregulated in T2D participants with DPN (Fig. 4B). Next, seven machine learning algorithms assessed the importance of the eight metabolites in T2D to DPN status (Fig. 4C). The RF machine learning algorithm had the highest AUC of 0.88, followed by GBM with AUC of 0.87, indicating they had the greatest predictive power for determining metabolite importance. Isoursodeoxycholate sulfate had the highest level of agreement across six machine learning algorithms. RF and GBM assigned a high importance score to six of the eight metabolites,

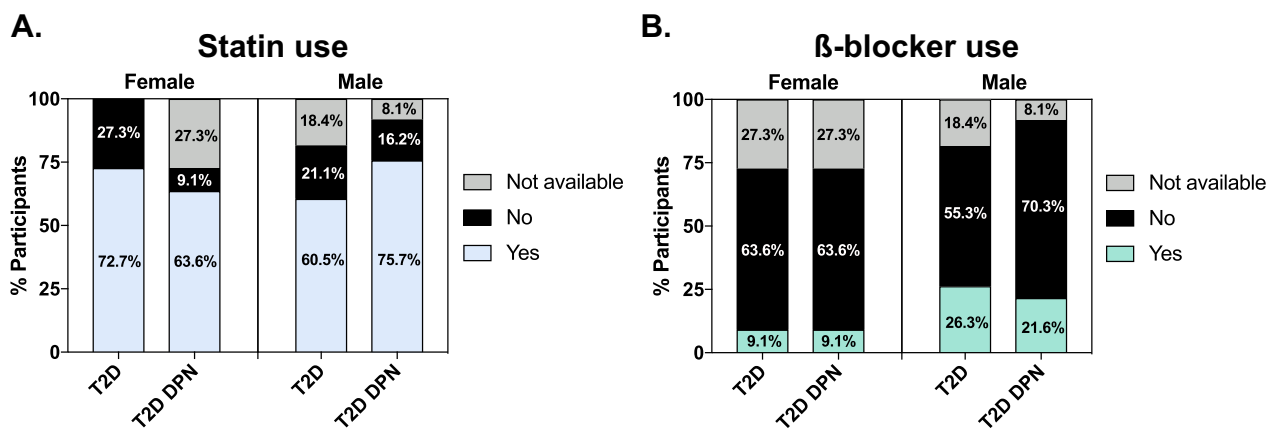


Figure 1. Medications prescribed to T2D participants in the study cohort. The percentage of type 2 diabetes participants (T2D) and T2D DPN participants (T2D DPN) treated with statins (A) or β -blockers (B) at the time of plasma collection. Most T2D participants without DPN and T2D participants with DPN were prescribed statins. Fewer T2D participants without DPN (9.1% female, less than 26.3% male) and T2D participants with DPN (9.1% female; 21.6% male) received β -blockers.

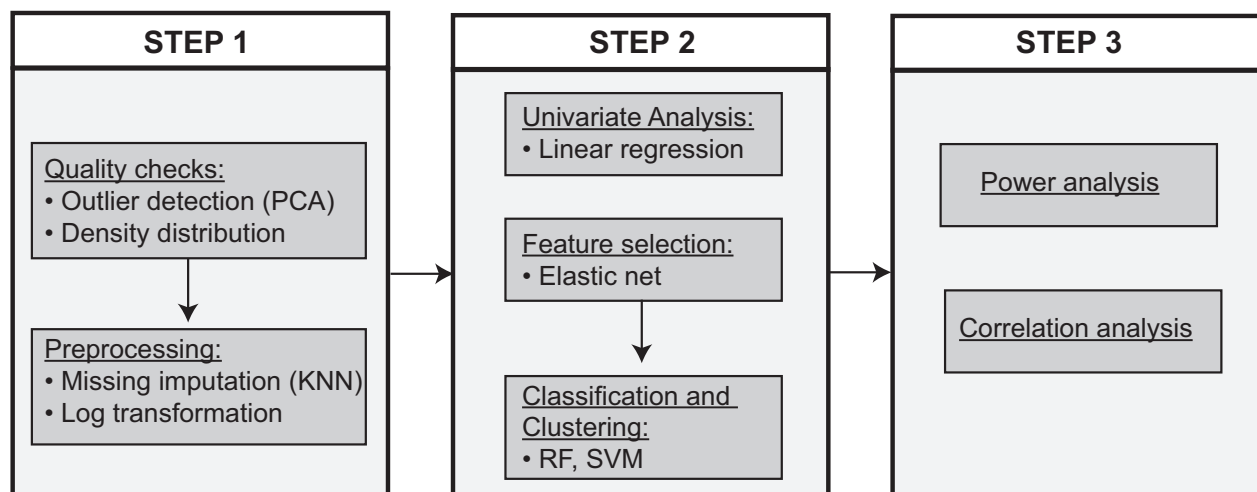


Figure 2. Bioinformatics pipeline used to identify plasma metabolites that associate with DPN in T2D. Step 1 included quality checks using principal component analysis (PCA), missing imputation using KNN, and log transformation. Step 2 focused on biomarker discovery by univariate and multivariate analysis, and machine learning algorithms. Step 3 performed power analysis to identify the metabolites contributing the most to the separation of T2D participants by DPN status. It also employed a correlation analysis to identify interconnectivity between the top elastic net plasma metabolites to lipid alterations associated with DPN in T2D. KNN, K-Nearest Neighbors; PCA, principal component analysis; RF, random forest; SVM, support vector machine.

suggesting they contributed strongly to the separation between T2D and T2D DPN participants. The six metabolites were isoursodeoxycholate sulfate, N-acetyl-3-methylhistidine, tartrate, citrate, N-acetyl- β -alanine, and ximenoylcarnitine (C26:1). The elastic net regression identified three metabolites (N-acetyl- β -alanine, ximenoylcarnitine (C26:1), and perfluorooctanoate) that differed significantly between T2D and T2D DPN participant groups and were not selected in the linear regression. Therefore, linear regression identified 12 metabolites and the elastic net analysis identified three

new metabolites totaling 15 metabolites that differed between T2D and T2D DPN. Boxplots of the relative abundance of the metabolites that differed across participant groups are provided in Figure S2.

Plasma metabolites differentially correlate with lipid species in T2D participants by DPN status

Five of the eight elastic net metabolites are reported to impact lipid and mitochondrial metabolism;^{22–26} thus, we

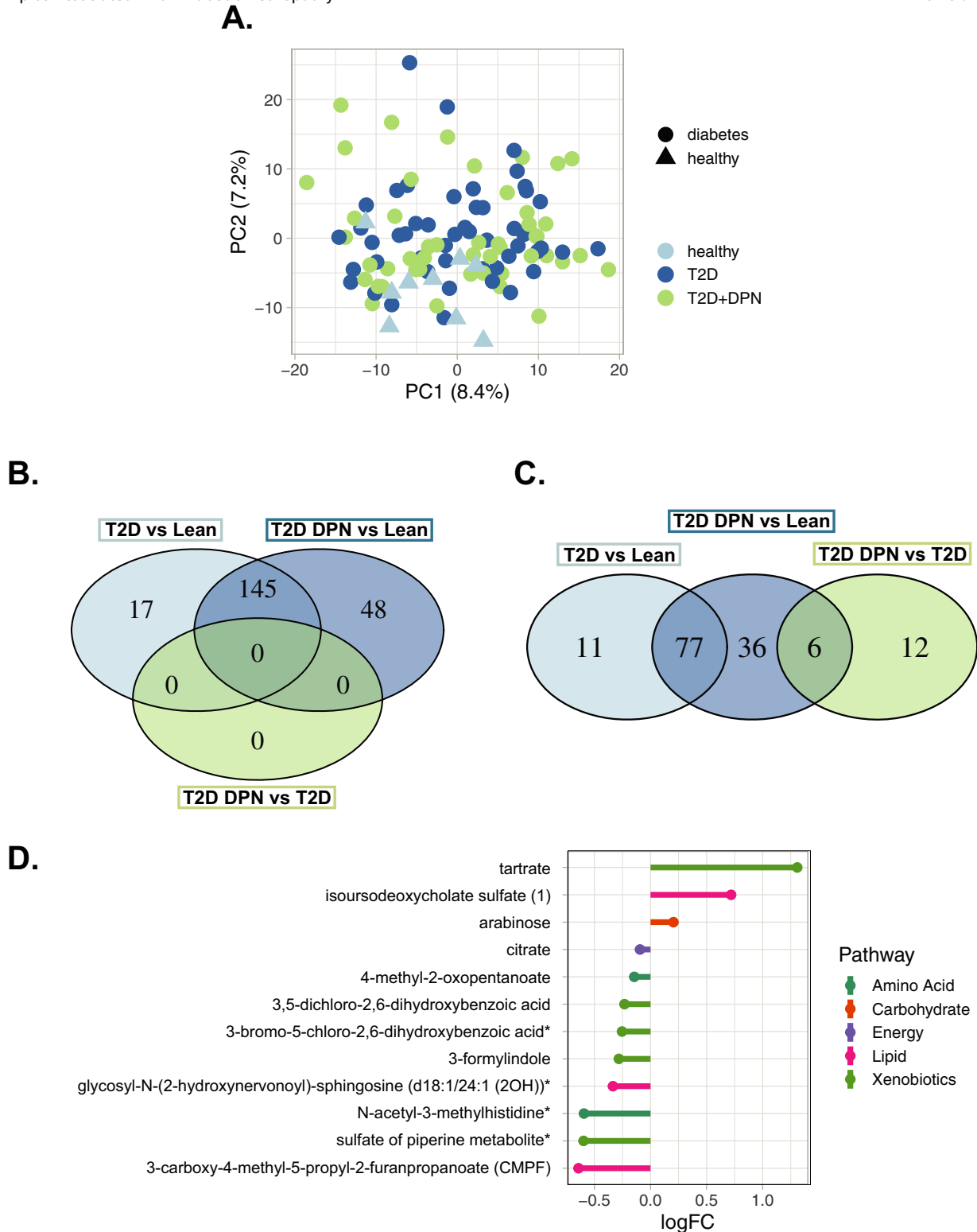


Figure 3. Linear regression identified differences in metabolites in plasma from lean control, T2D, and T2D DPN participants. (A) PCA plot of metabolites separated by lean control, T2D, or T2D DPN participant groups. (B) Venn diagram depicting the number of significant metabolites that are unique or shared across all groups ($Q < 0.05$) from an unadjusted t -test analysis. (C) Venn diagram of the number of significant shared and unique metabolites across groups ($p < 0.05$) determined by a linear regression model adjusted for age, sex, and medications. (D) Log fold-change (FC) of the 12 unique metabolites differentially regulated between T2D participants with and without DPN. Metabolites marked by asterisks (*) represent uncertainties in metabolite quantification and identification. PCA, principal component analysis, Sulfate of piperine metabolite, formula $C_{16}H_{19}NO_3$ (3).

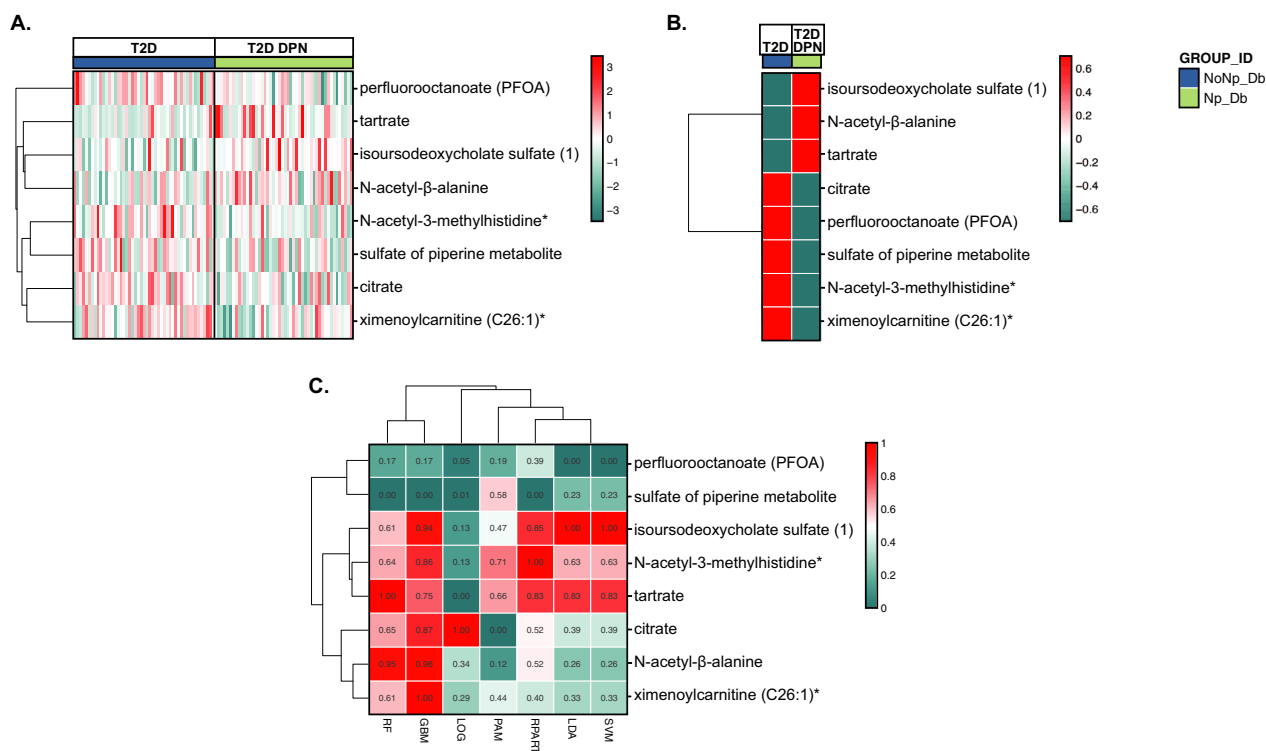


Figure 4. Elastic net analysis identified eight unique metabolites that differentiate T2D participants by DPN status. (A) The relative abundance of the eight elastic net metabolites in individual participants with T2D (left) and T2D DPN (right) plotted as a heat map. (B) The relative abundance of the eight metabolites from T2D participants (left) and T2D DPN participants (right) were averaged and displayed as a mean value. (C) Seven different machine learning algorithms were trained to classify T2D and T2D DPN using the eight elastic net metabolites. The importance scores of elastic net metabolites were extracted from seven different machine learning models, including Random Forest (RF), Gradient Boosting Machine (GBM), Logistic Regression (LOG), Prediction Analysis for Microarrays (PAM), Recursive Partitioning and Regression Trees (RPART), Linear Discriminant Analysis (LDA), and Support Vector Machine (SVM). The importance scores represent the contribution of metabolites to the performance of the machine learning model. Importance scores range from 0 representing “no importance” to 1 representing “high importance”. Metabolites marked by asterisks (*) represent uncertainties in metabolite quantification and identification. Sulfate of piperine metabolite, formula $C_{16}H_{19}NO_3$ (3).

conducted a correlation analysis to explore connections between these eight plasma metabolites to changes in the plasma lipid profile of T2D participants by DPN status (Fig. 5). We found significant correlations ($p < 0.05$) between the eight metabolites and 473 lipid species in T2D participants, of which 86 lipid species are depicted (Fig. 5). There were more connections between the eight metabolites and lipid species in T2D participants with DPN versus without DPN, especially between ximenoylcarnitine (C26:1), isoursodeoxycholate sulfate, and citrate. These metabolites connected to several lipids, suggesting these metabolite-lipid correlations associate with T2D DPN. For example, isoursodeoxycholate sulfate negatively associated with sphingomyelins, citrate positively associated with metabolites of fatty acid metabolism, and ximenoylcarnitine (C26:1) with many glycerophospholipid and acylcarnitine species.

Plasma lipid abundance, chain length, and saturation in T2D participants correlate to DPN status

The association between the top eight metabolites and alterations in specific lipid species motivated us to investigate changes in abundance, chain length, and saturation degree for all lipids from the metabolomics analysis (Fig. 6). The global metabolomics platform we used detects a broad range of polar and neutral lipid classes, allowing us to assess alterations across lipid classes. The free fatty acid (FFA) plasma profile from lean participants showed high levels of very long-chain fatty acids greater than 19 carbons in length and several species of medium-chain fatty acids. Conversely, plasma from T2D participants with or without DPN was characterized by an accumulation of medium- and long-chain saturated fatty acids

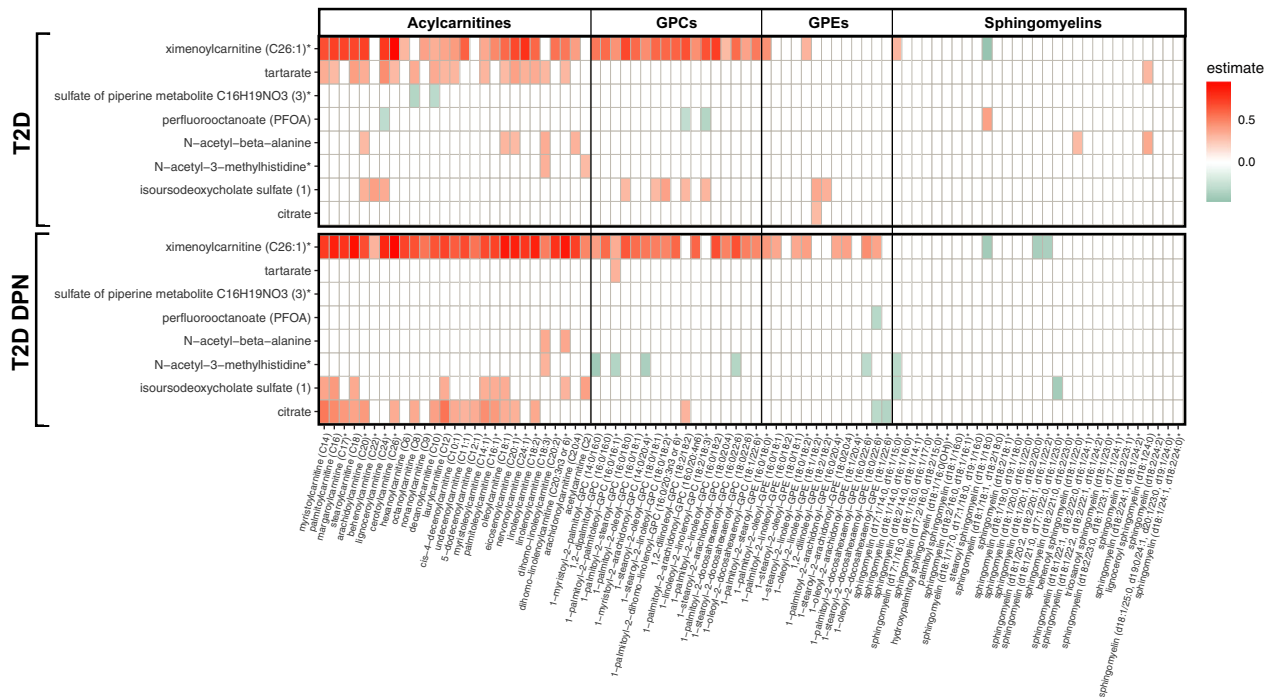


Figure 5. Correlation analysis shows associations between elastic net to lipid metabolites. Heat map of Spearman correlations ($p < 0.05$) was used to assess associations between the eight elastic net metabolites to all lipid metabolites. Plasma from T2D participants and T2D DPN participants show positive correlations (red) and negative correlations (green) between lipids.

(LCSFAs) ranging from 8 to 18 carbons in length (Fig. 6A). Among complex lipids, T2D plasma contained elevated levels of diacylglycerols (DAGs) and phosphatidylethanolamines (PEs) but lower levels of phosphatidylcholines (PCs) compared to lean participants (Fig. 6B). Importantly, there was a decrease in all plasma acylcarnitines, ceramides, and sphingomyelins (SMs) in T2D participants compared to healthy controls (Fig. 6C). Changes in all complex lipid abundance were even more pronounced in T2D DPN participants versus controls (Fig. 6A–C). Particularly, T2D DPN plasma was marked by a significant reduction in two acylcarnitine species [ximenoylcarnitine (26:1), lignoceroylcarnitine (24:0)] and one sphingolipid intermediate [glycosyl-N-(2-hydroxynervonoyl)-sphingosine (d18:1/24:1(2OH))] compared to T2D participants without polyneuropathy (Fig. 6D). These results suggest that changes to the plasma lipid profile correlate with DPN in T2D (Fig. 7).

Discussion

We conducted an explorative global plasma metabolomics analysis on participants with screen-detected T2D from ADDITION-Denmark to identify circulating metabolites that correlate with DPN diagnosed at a follow-up appointment a mean of 13 years after T2D

diagnosis.^{7,10} As expected, T2D status strongly influenced the plasma metabolite profile compared to lean controls, although we also identified unique metabolites associated with DPN status among the T2D participants. Several of these metabolites relate to metabolically active lipid pathways. We also found that T2D and DPN status produced changes in lipid abundance, chain length, and saturation for plasma FFA and complex lipids, including DAGs, sphingolipids, and acylcarnitines. Collectively, these results suggest that plasma metabolite profiles related to complex lipid metabolism are linked to DPN in T2D, and may provide insight into DPN pathogenesis.

In this study, our cohort was age- and sex-matched across T2D, T2D DPN, and lean groups. The diabetes groups exhibited the anticipated metabolic characteristics, for example, elevated HbA1c, glucose, BMI, waist circumference, which were observed in similar cohorts.^{7,27,28} Basic plasma lipid characteristics in the diabetes group revealed lower total cholesterol compared to lean controls, presumably due to statin use. Diabetes participants also had nonsignificant increases in triglycerides and decreases in HDL, despite taking statins. This is possibly due to β -blocker use, which can result in trending increases in plasma triglycerides.^{21,29} Although uncontrolled hyperglycemia² and dyslipidemia²⁰ are DPN risk factors, we did

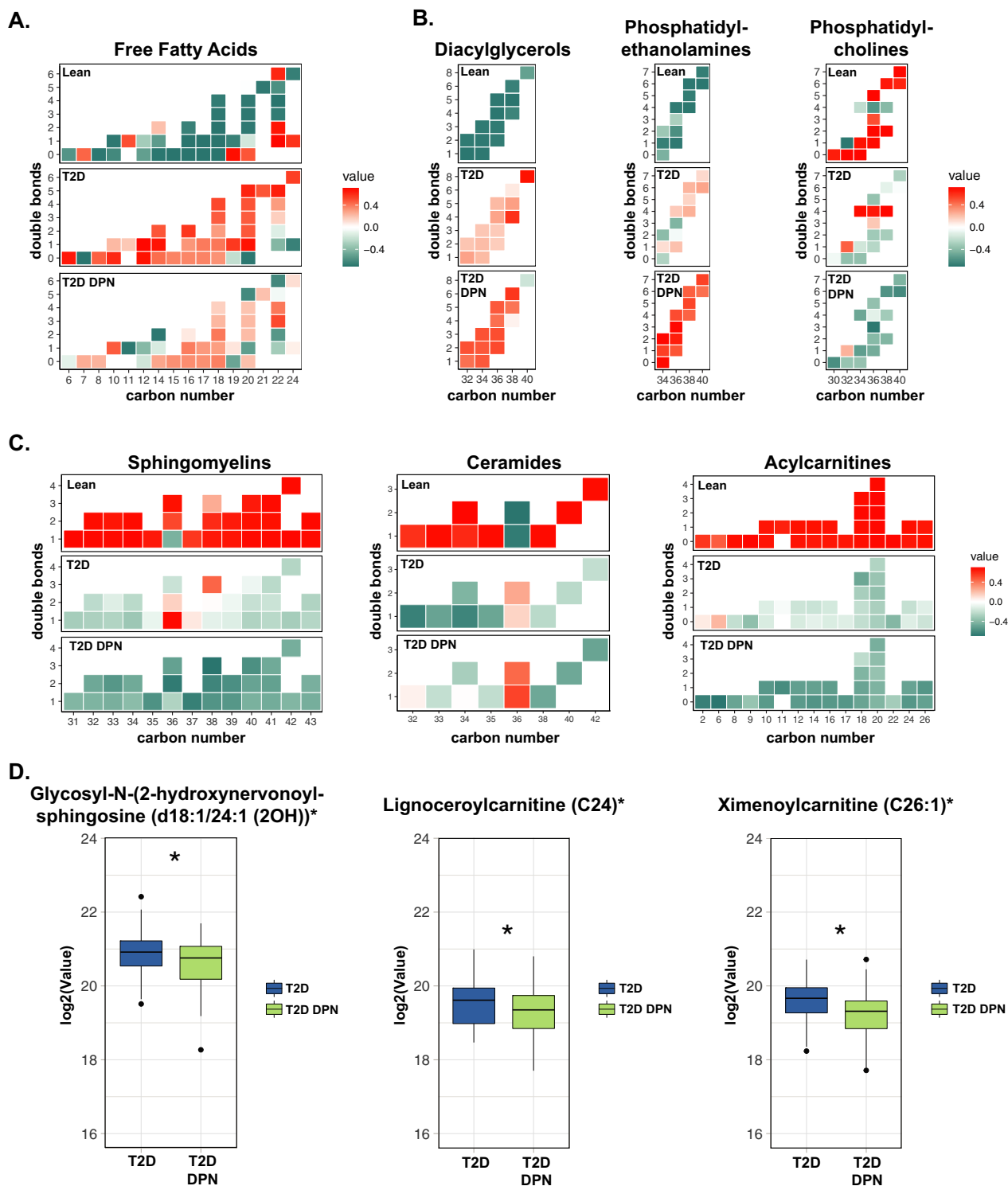


Figure 6. Plasma free fatty acid and complex lipid abundance, chain length, and saturation level in lean control, T2D, and T2D DPN participants. (A) Heat maps of free fatty acid profiles in plasma from lean control, T2D, and T2D DPN participants show altered chain length and saturation of free fatty acids. (B) Heat maps of complex lipids show increases in DAGs and PEs while PCs decrease in T2D participants. (C) SM, ceramide, and acylcarnitine metabolites also show alterations in lean control, T2D, and T2D DPN participants. (D) Two acylcarnitine metabolites and one sphingolipid metabolite were significantly altered in T2D DPN patients versus T2D without DPN; * $p < 0.05$.

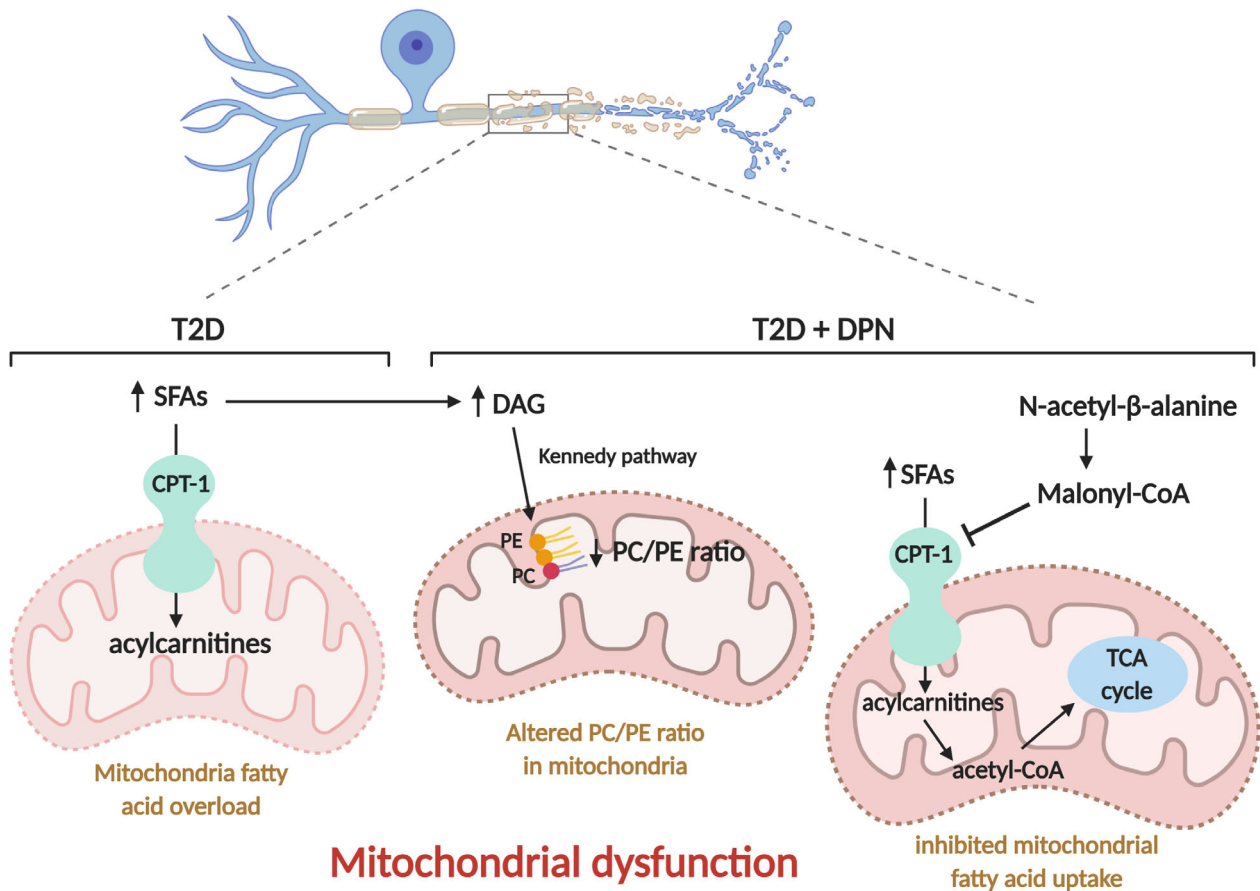


Figure 7. Proposed mechanism for the effect of plasma metabolites on mitochondrial function within the nerve. The metabolites and lipids altered in T2D DPN versus T2D participants may induce mitochondrial dysfunction through three pathways. First, the shift from very long-chain and medium-chain fatty acids to LCSFAs in T2D participant plasma likely leads to mitochondrial bioenergetics overload. Second, elevated N-acetyl-β-alanine levels may induce higher malonyl-CoA production and block CPT-1, which would reduce acylcarnitine levels and mitochondrial ATP production, triggering mitochondrial dysfunction. Reductions in acylcarnitine and citrate levels may also impair the TCA cycle, reducing mitochondrial ATP production. Third, elevated DAG levels stimulate de novo PE and PC synthesis. Alterations in the PC:PE ratio in the mitochondrial membrane may also lead to mitochondrial dysfunction. CPT-1, carnitine palmitoyltransferase-1; DAGs, diacylglycerols; LCSFAs, long-chain saturated fatty acids; PCs, phosphatidylcholines; PEs, phosphatidylethanolamines; TCA, the citric acid cycle.

not observe significant differences in any metabolic metric in T2D participants with or without DPN. However, there were trends that agreed with other cross-sectional studies of T2D participants with DPN.^{5,30–33} Additionally, statin use, which influences the lipid profile, did not affect DPN risk in another Danish cohort.⁸ Thus, we hypothesized that alterations in specific lipid or metabolite species may underlie DPN, rather than dyslipidemia or hypertriglyceridemia *per se*, in this patient cohort.⁸

This led to our global plasma metabolomics analysis of control, T2D, and T2D DPN participants to identify specific differential metabolites and lipids by DPN status. Age-, sex-, and medication use-adjusted univariate linear regression and multivariate elastic net selected 12 and 8 metabolites, respectively. Three metabolites, isoursodeoxycholate (a secondary bile acid), 3-formylindole (an L-

tryptophan metabolite), and CMPF (a metabolite of furan fatty acids) are metabolized by gut microbiota suggesting a link between DPN and the gut microbiome.²³ We found that isoursodeoxycholate, which modulates lipid absorption and belongs to the Lipid super-pathway, positively associated with DPN status. In the KORA FF4 study, fecal isoursodeoxycholate correlated positively with serum triglycerides;²³ indeed, herein, the T2D DPN group, which had elevated plasma isoursodeoxycholate, also had a trending increase in triglycerides versus T2D participants without DPN. CMPF, another member of the Lipid super-pathway, could also be related to microbial action in the gut through furan fatty acid breakdown.³⁴ Elevated CMPF correlates with T2D and β-cell dysfunction,^{35,36} although there are no conclusive studies on the effect of CMPF on DPN. Overall, the metabolite findings in this

study strongly support future studies focused on the role of gut microbiota in DPN.

Many selected metabolites belong to the Xenobiotics super-pathway. One notable example is PFOA, previously linked in preclinical studies to mitochondrial uncoupling,³⁷ mitochondrial dysfunction,²⁶ and impaired glucose homeostasis.³⁸ Epidemiological studies report conflicting findings on PFOA exposure as a potential risk factor for T2D development or associated microvascular complications, although this may be due to population-specific attributes or PFOA isomers.³⁹ Herein, PFOA was lower in T2D DPN versus T2D participants, which suggests it does not affect diabetes complications, or DPN at least. These findings agree with our preclinical DPN prevention study using another mitochondrial uncoupler, niclosamide ethanolamine, which had no therapeutic effect on DPN in a T2D mouse model.⁴⁰ Since participants are exposed to a multitude of complex exogenous and endogenous xenobiotics,⁴¹ correlations between xenobiotics and participant groups may be unreliable due to the small number of participants in this cohort and will require further evaluation.

Metabolites differentiated by DPN status were also related to energy [citrate, tricarboxylic acid cycle (TCA)] and lipid metabolism [CMPF, ximenoylcarnitine (C26:1), glycosyl-N-(2-hydroxynervonoyl)-sphingosine (d18:1/24:1 (2OH))]. Impaired energy homeostasis and mitochondrial dysfunction are associated with T2D and diabetic complications, including DPN.^{42,43} Citrate, a crucial mitochondrial TCA intermediate, was significantly lower in plasma from T2D DPN participants, paralleling our studies in sciatic nerve from T2D DPN mice, which were deficient in both glycolytic and TCA intermediates, including citrate.^{24,44} Mitochondria are the primary site of lipid metabolism, generating acetyl-CoA through fatty acid β -oxidation, which feeds into the TCA cycle. Alternatively, citrate in the cytosol can serve as a precursor for fatty acid synthesis and has been reported to contribute to de novo lipogenesis in models of insulin resistance⁴⁵ and diabetic complications.⁴⁶ Cytosolic citrate cleaved by ATP-citrate lyase produces oxaloacetate and acetyl-CoA. Acetyl-CoA is then converted into malonyl-CoA by acetyl-CoA carboxylase, a committed step in fatty acid synthesis, which stimulates de novo lipogenesis.⁴⁷ Moreover, complex metabolically active lipids also dictate mitochondrial structure and function through membrane curvature.⁴⁸

Metabolites belonging to amino acid metabolism [including 4-methyl-2-oxopentanoate, branched chain amino acid (BCAA) metabolism], carbohydrate metabolism (arabinose, pentose metabolism), and nucleotide metabolism (N-acetyl- β -alanine) were also identified. We found 4-methyl-2-oxopentanoate, which is derived from L-leucine

and feeds into BCAA metabolism, was lower in T2D participants with DPN. Clinical studies have shown that BCAA pathway alterations are a risk for incident T2D.⁴⁹ Here, the results suggest BCAA metabolism, which can affect mitochondrial function, glucose metabolism, and insulin sensitivity,^{50,51} may also be linked to DPN status. Elevated N-acetyl- β -alanine levels, as observed in our study, may similarly alter the TCA cycle and impair mitochondrial energy production,²⁵ which could lead to nerve injury. Importantly, when correcting for the analysis of multiple comparisons by evaluating *Q*-values, we found that many of the significant metabolites may potentially be false discoveries. While our significant metabolite profiles agree with several previous studies in patients with T2D,^{23,39,46,50,52} future studies, with larger sample sizes are needed to confirm our findings.

Since we identified many metabolites centered around mitochondrial metabolism and lipids, we next determined the connectivity between the eight T2D DPN metabolites identified by elastic net and plasma lipid metabolites. Interestingly, citrate correlated positively with several acylcarnitines in plasma from T2D DPN participants, but not those without DPN. Similarly, ximenoylcarnitine (C26:1) had more correlations with acylcarnitines and glycerophospholipids in T2D DPN versus T2D participants without DPN. We previously reported alterations in glycerophospholipid metabolism in the sciatic nerve of neuropathic T2D murine models, suggesting glycerophospholipid metabolism may be dysregulated by T2D in both humans and mice.⁵³ In light of these differences dictated by DPN status, we evaluated changes in abundance, chain length, and saturation degree of plasma FFAs and complex lipids. While there were only 12 and 8 metabolites that significantly differed by DPN status in the univariate and multivariate analysis, respectively, we hypothesized that the high connectivity between the metabolites and lipid species was indicative of broader lipidomic changes across lipid classes.

FFAs were distinctly impacted by T2D status. The FFA profile shifted from medium and very long-chain polyunsaturated fatty acids in lean participants to an abundance of long-chain saturated fatty acids in T2D, regardless of DPN status, as previously reported.⁵⁴ With regard to complex lipids, there was an increase in DAGs and PEs and a decrease in PCs, SMs, and ceramides comprising long-chain FAs (containing 30–43 carbons in sum) in T2D plasma. Changes in complex lipid fatty acyl chain length and saturation alter cellular processes in T2D by impacting signaling pathways, mitochondrial β -oxidation, subcellular localization, and membrane fluidity and curvature.⁵⁵ The rise we observed in plasma DAGs is well established in T2D. DAGs are precursors for triglyceride synthesis by diacylglycerol transferase 2 (DGAT2), which is increased in sural and sciatic nerve from

humans and mice, respectively, with T2D DPN.⁵³ DAGs are also important signaling molecules that activate the family of protein kinase C (PKC) enzymes, which are involved in a wide range of biological vascular functions.⁵⁶ Despite this central role in diabetic complications, blocking PKC activity does not consistently improve DPN in clinical trials.⁵⁷

DAGs are also converted into PEs and PCs through the de novo Kennedy pathway, by condensation of cytidine 5'-diphosphate (CDP)-ethanolamine and CDP-choline, respectively.⁵⁸ The increased PEs and decreased PCs in T2D participant plasma in our study resulted in a drop in PE:PC ratio. The drop in PE:PC ratio was steeper in our DPN cohort, suggesting altered mitochondrial function, possibly at the neural level, in T2D DPN participants. PCs and PEs are the most abundant mitochondrial phospholipids, and changes to the PC:PE ratio disrupts mitochondrial respiration and ATP production.⁴⁸ Indeed, we have shown that dyslipidemic conditions impair mitochondrial respiratory capacity⁵⁹ and ATP production^{60,61} in cultured sensory neurons. Additionally, genes related to mitochondrial dysfunction are upregulated within the sciatic nerve of T2D DPN mouse models.⁶²

We also found that SM and ceramide metabolites were reduced in plasma from all T2D participants, consistent with earlier studies.^{52,63} As with the PC and PE trend, the most pronounced changes were in the DPN cohort. Low plasma SM levels may correlate with poorer neurological outcomes.⁶⁴ Moreover, ablating sphingomyelin synthase 1 in mice reduces ATP production and increases reactive oxygen generation in β -cell mitochondria.⁶⁵ Reduced plasma SMs could result from lower lipoprotein cholesterol^{7,66} or a decrease in SM synthesis from a deficiency of sphingolipid intermediates, such as glycosyl-N-(2-hydroxynervonoyl)-sphingosine (d18:1/24:1(2OH)), which was significantly lower in T2D DPN plasma in this study.

We observed that acylcarnitines ranging in chain lengths between 2 and 26 were also decreased in T2D, indicating a reduction in all acylcarnitine fatty acids. The decrease in long-chain acylcarnitines in T2D DPN participants agrees with our recent findings in a T2D cohort of American Indians with DPN⁶⁷ and diabetic nephropathy.⁴⁶ It is possible that the elevated plasma levels we observed of N-acetyl- β -alanine, a precursor to malonyl-CoA, inhibited carnitine palmitoyltransferase 1 (CPT-1).⁶⁸ Since CPT-1 catalyzes long-chain acylcarnitine formation from long-chain fatty acyl-CoAs, CPT-1 inhibition by malonyl-CoA may reduce plasma acylcarnitine levels.⁶⁸ Alternatively, β -alanine can cause oxidative stress and decrease ATP levels, and impair mitochondrial function in embryonic fibroblasts,²⁵ a mechanism that may also drive mitochondrial dysfunction associated with DPN in T2D.

Overall, the pattern in complex lipid abundance in all T2D versus control participants intensified when the T2D

cohort was stratified by DPN status. Collectively, these novel lipid findings support a mechanism whereby a shift from unsaturated fatty acids to LCSFAs as mitochondrial fuel within the nerve triggers mitochondrial dysfunction (Fig. 7).^{59–61} Elevated N-acetyl- β -alanine levels in T2D DPN participants may worsen mitochondrial dysfunction by impairing the TCA cycle or triggering the formation of malonyl-CoA, a potent CPT-1 inhibitor. CPT-1 inhibition by malonyl-CoA significantly reduces acylcarnitine formation and ATP production by mitochondrial β -oxidation. This loss of acylcarnitines as a mitochondrial energy substrate could impair β -oxidation, resulting in energy failure, which could contribute to DPN. The reduction in sphingolipid intermediates also indicates that disrupted sphingolipid synthesis pathways may reduce SMs and ceramides in the nerve, contributing to T2D DPN. Collectively, these changes may lead to mitochondrial dysfunction and energy depletion with resulting nerve injury.

This study had limitations. The lean control group was small, which limited our power to detect potentially important metabolite differences between the groups. Our cohort consisted of a disproportionate number of male versus female participants in each group, which prevented us from evaluating the contribution of sex differences to plasma metabolomics and the large number of comparisons made across participant groups could have resulted in false-positive discoveries. While we applied the rigorous statistical methodology to limit this possibility, our results need to be validated in larger T2D cohorts. Finally, our DPN definition did not incorporate symptoms or examination features, which may have led to misclassification bias. Our DPN definition, however, utilized comprehensive NCS parameters, which have strong diagnostic characteristics.¹¹

In conclusion, plasma from T2D DPN participants exhibited altered lipid and metabolite levels, which are centered around lipid metabolism and mitochondrial function. This study has important clinical implications for T2D patients and suggests that dysfunctional lipid metabolism is associated with T2D DPN. This exploratory untargeted metabolomics analysis also revealed potential links to microbiome and xenobiotic exposure. Future directions could focus on exogenous (e.g., microbiome, exposome) and endogenous factors that regulate complex lipid pathways, the importance of carbon chain length, and testing of our proposed mechanism to identify potential therapeutic T2D DPN targets, which currently lack any tangible effective therapies.

Acknowledgments

This study is part of the International Diabetic Neuropathy Consortium research program. This work was

supported by the Novo Nordisk Foundation through a Novo Nordisk Foundation Challenge Programme grant [grant number NNF14OC0011633]; the National Institutes of Health [grant numbers 1R24DK082841, 1R21NS102924, 1DP3DK094292, 1F32DK112642, 1K99DK119366, and T32NS0007222]; the American Diabetes Association [grant number 7-12-BS-045]; the NeuroNetwork for Emerging Therapies; and the A. Alfred Taubman Medical Research Institute. The authors thank Dr. Bhumsoo Kim for generating Figure 7 and Metabolon for conducting the global plasma metabolomics analysis.

Authors' Contributions

AER, KG, FMA, STA, and ELF designed research; STA and ELF performed research; STA, MEJ, DRW, HT, MC, and BCC performed neurophysiological examinations; TSJ contributed to the clinical examination of participants and edited the manuscript; AER, KG, FMA, ELR, MGS, and ELF analyzed data; AER, KG, ELR, MGS, and ELF wrote the paper; AER, KG, ELR, MGS, and ELF edited the paper. All authors read, revised, and approved the submitted manuscript.

Conflict of Interest

AER and ELR were supported by grants from the National Institutes of Health during this study. MEJ reports grants from Astra Zeneca, Sanofi Aventis, Boehringer Ingelheim, AMGEN, Novo Nordisk, and hold shares in Novo Nordisk outside the submitted work. BCC received grants from the NIDDK, Veterans Affairs, JDRE, and the American Academy of Neurology as well as personal fees from PCORI, Medical legal work, DynaMed, Vaccine Injury Compensation Program, and the American Academy of Neurology separate from this study. MC reports personal fees from Novo Nordisk A/S and Boehringer Ingelheim A/S during the conduct of the study. TSJ reports grants from Novo Nordisk Foundation during the study. ELF received grants from the National Institutes of Health, the American Diabetes Association, the NeuroNetwork for Emerging Therapies, and the A. Alfred Taubman Medical Research Institute during the conduct of the study.

References

- Feldman EL, Callaghan BC, Pop-Busui R, et al. Diabetic neuropathy. *Nat Rev Dis Primers* 2019;13:41.
- Callaghan BC, Little AA, Feldman EL, Hughes RA. Enhanced glucose control for preventing and treating diabetic neuropathy. *Cochrane Database Syst Rev* 2012;6:CD007543.
- Callaghan BC, Gao LL, Li Y, et al. Diabetes and obesity are the main metabolic drivers of peripheral neuropathy. *Ann Clin Transl Neurol* 2018;5:397–405.
- Callaghan BC, Hur J, Feldman EL. Diabetic neuropathy: one disease or two? *Curr Opin Neurol* 2012;25:536–541.
- Callaghan BC, Xia R, Banerjee M, et al. Metabolic syndrome components are associated with symptomatic polyneuropathy independent of glycemic status. *Diabetes Care* 2016;39:801–807.
- Alberti K, Eckel RH, Grundy SM, et al. Harmonizing the metabolic syndrome: a joint interim statement of the International Diabetes Federation Task Force on Epidemiology and Prevention; National Heart, Lung, and Blood Institute; American Heart Association; World Heart Federation; International Atherosclerosis Society; and International Association for the Study of Obesity. *Circulation* 2009;20:1640–1645.
- Andersen ST, Witte DR, Dalsgaard E-M, et al. Risk factors for incident diabetic polyneuropathy in a cohort with screen-detected type 2 diabetes followed for 13 years: ADDITION-Denmark. *Diabetes Care* 2018;41:1068–1075.
- Kristensen FP, Christensen DH, Callaghan BC, et al. Statin therapy and risk of polyneuropathy in type 2 diabetes: a Danish Cohort Study. *Diabetes Care* 2020;43:2945–2952.
- Lauritzen T, Griffin S, Borch-Johnsen K, et al. The ADDITION study: proposed trial of the cost-effectiveness of an intensive multifactorial intervention on morbidity and mortality among people with Type 2 diabetes detected by screening. *Int J Obes Relat Metab Disord* 2000;24(Suppl 3):S6–S11.
- Sandbæk A, Griffin SJ, Sharp SJ, et al. Effect of early multifactorial therapy compared with routine care on microvascular outcomes at 5 years in people with screen-detected diabetes: a randomized controlled trial: the ADDITION-Europe Study. *Diabetes Care* 2014;37:2015–2023.
- Dyck PJ, Carter RE, Litchy WJ. Modeling nerve conduction criteria for diagnosis of diabetic polyneuropathy. *Muscle Nerve* 2011;44:340–345.
- Beretta L, Santaniello A. Nearest neighbor imputation algorithms: a critical evaluation. *BMC Med Inform Decis Mak* 2016;16(Suppl 3):74.
- Worley B, Powers R. Multivariate analysis in metabolomics. *Curr Metabolomics* 2013;1:92–107.
- Storey JD. A direct approach to false discovery rates. *J Roy Stat Soc Ser B* 2002;64:479–498.
- Storey JD, Taylor JE, Siegmund D. Strong control, conservative point estimation and simultaneous conservative consistency of false discovery rates: a unified approach. *J Roy Stat Soc Ser B* 2004;66:187–205.
- Paolino JP. Rasch model parameter estimation via the elastic net. *J Appl Meas* 2015;16:353–364.
- Al-Akwaa FM, Yunits B, Huang S, et al. Lilikoi: an R package for personalized pathway-based classification modeling using metabolomics data. *Gigascience* 2018;1:7.
- Kuhn M. Building Predictive Models in R Using the caret Package. *J Stat Softw* 2008;28:1–26.

19. Robin X, Turck N, Hainard A, et al. pROC: an open-source package for R and S+ to analyze and compare ROC curves. *BMC Bioinformatics* 2011;17:77.
20. Wiggin TD, Sullivan KA, Pop-Busui R, et al. Elevated triglycerides correlate with progression of diabetic neuropathy. *Diabetes* 2009;58:1634–1640.
21. Bell DS. Advantages of a third-generation beta-blocker in patients with diabetes mellitus. *Am J Cardiol* 2004;93:49B–52B.
22. Arcaro CA, Gutierrez VO, Assis RP, et al. Piperine, a natural bioenhancer, nullifies the antidiabetic and antioxidant activities of curcumin in streptozotocin-diabetic rats. *PLoS One* 2014;9:e113993.
23. Breuninger TA, Wawro N, Meisinger C, et al. Associations between fecal bile acids, neutral sterols, and serum lipids in the KORA FF4 study. *Atherosclerosis* 2019;288:1–8.
24. Sas KM, Kayampilly P, Byun J, et al. Tissue-specific metabolic reprogramming drives nutrient flux in diabetic complications. *JCI Insight* 2016;22:e86976.
25. Shetewy A, Shimada-Takaura K, Warner D, et al. Mitochondrial defects associated with beta-alanine toxicity: relevance to hyper-beta-alaninemia. *Mol Cell Biochem* 2016;416:11–22.
26. Suh KS, Choi EM, Kim YJ, et al. Perfluorooctanoic acid induces oxidative damage and mitochondrial dysfunction in pancreatic beta-cells. *Mol Med Rep* 2017;15:3871–3878.
27. Andersen ST, Witte DR, Andersen H, et al. Risk-factor trajectories preceding diabetic polyneuropathy: ADDITION-Denmark. *Diabetes Care* 2018;41:1955–1962.
28. Määttä LL, Charles M, Witte DR, et al. Prospective study of neuropathic symptoms preceding clinically diagnosed diabetic polyneuropathy: ADDITION-Denmark. *Diabetes Care* 2019;42:2282–2289.
29. Fogari R, Zoppi A, Corradi L, et al. Beta-blocker effects on plasma lipids during prolonged treatment of hypertensive patients with hypercholesterolemia. *J Cardiovasc Pharmacol* 1999;33:534–539.
30. Callaghan BC, Xia R, Reynolds E, et al. Association between metabolic syndrome components and polyneuropathy in an obese population. *JAMA Neurol* 2016;1:1468–1476.
31. Han L, Ji L, Chang J, et al. Peripheral neuropathy is associated with insulin resistance independent of metabolic syndrome. *Diabetol Metab Syndr* 2015;7:14.
32. Hanewinkel R, Drenthen J, Ligthart S, et al. Metabolic syndrome is related to polyneuropathy and impaired peripheral nerve function: a prospective population-based cohort study. *J Neurol Neurosurg Psychiatry* 2016;87:1336–1342.
33. Savelieff MG, Callaghan BC, Feldman EL. The emerging role of dyslipidemia in diabetic microvascular complications. *Curr Opin Endocrinol Diabetes Obes* 2020;27:115–123.
34. Xu L, Sinclair AJ, Faiza M, et al. Furan fatty acids - beneficial or harmful to health? *Prog Lipid Res* 2017;68:119–137.
35. Liu Y, Prentice K, Eversley J, et al. Rapid elevation in CMPF may act as a tipping point in diabetes development. *Cell Rep* 2016;29:2889–2900.
36. Prentice KJ, Luu L, Allister EM, et al. The furan fatty acid metabolite CMPF is elevated in diabetes and induces beta cell dysfunction. *Cell Metab* 2014;1:653–666.
37. Shabalina IG, Kalinovich AV, Cannon B, Nedergaard J. Metabolically inert perfluorinated fatty acids directly activate uncoupling protein 1 in brown-fat mitochondria. *Arch Toxicol* 2016;90:1117–1128.
38. Du G, Sun J, Zhang Y. Perfluorooctanoic acid impaired glucose homeostasis through affecting adipose AKT pathway. *Cytotechnology* 2018;70:479–487.
39. Cardenas A, Hivert M-F, Gold DR, et al. Associations of perfluoroalkyl and polyfluoroalkyl substances with incident diabetes and microvascular disease. *Diabetes Care* 2019;42:1824–1832.
40. Hinder LM, Sas KM, O'Brien PD, et al. Mitochondrial uncoupling has no effect on microvascular complications in type 2 diabetes. *Sci Rep* 2019;29:881.
41. Southam AD, Lange A, Al-Salhi R, et al. Distinguishing between the metabolome and xenobiotic exposome in environmental field samples analysed by direct-infusion mass spectrometry based metabolomics and lipidomics. *Metabolomics* 2014;10:1050–1058.
42. Hinder LM, Vincent AM, Burant CF, et al. Bioenergetics in diabetic neuropathy: what we need to know. *J Peripher Nerv Syst* 2012;17(Suppl 2):10–14.
43. Rumora AE, Savelieff MG, Sakowski SA, Feldman EL. Disorders of mitochondrial dynamics in peripheral neuropathy: clues from hereditary neuropathy and diabetes. *Int Rev Neurobiol* 2019;145:127–176.
44. Hinder LM, Vivekanandan-Giri A, McLean LL, et al. Decreased glycolytic and tricarboxylic acid cycle intermediates coincide with peripheral nervous system oxidative stress in a murine model of type 2 diabetes. *J Endocrinol* 2013;216:1–11.
45. Carlson CA, Kim KH. Regulation of hepatic acetyl coenzyme A carboxylase by phosphorylation and dephosphorylation. *Arch Biochem Biophys* 1974;164:478–489.
46. Afshinnia F, Nair V, Lin J, et al. Increased lipogenesis and impaired beta-oxidation predict type 2 diabetic kidney disease progression in American Indians. *JCI Insight* 2019;1:4.
47. Song Z, Xiaoli AM, Yang F. Regulation and metabolic significance of de novo lipogenesis in adipose tissues. *Nutrients* 2018;29:10.
48. Basu Ball W, Neff JK, Gohil VM. The role of nonbilayer phospholipids in mitochondrial structure and function. *FEBS Lett* 2018;592:1273–1290.

49. Guasch-Ferré M, Hruba A, Toledo E, et al. Metabolomics in prediabetes and diabetes: a systematic review and meta-analysis. *Diabetes Care* 2016;39:833–846.
50. Karusheva Y, Koessler T, Strassburger K, et al. Short-term dietary reduction of branched-chain amino acids reduces meal-induced insulin secretion and modifies microbiome composition in type 2 diabetes: a randomized controlled crossover trial. *Am J Clin Nutr* 2019;1:1098–1107.
51. Li T, Zhang Z, Kolwicz SC, et al. Defective branched-chain amino acid catabolism disrupts glucose metabolism and sensitizes the heart to ischemia-reperfusion injury. *Cell Metab* 2017;7:374–385.
52. Xu F, Tavintharan S, Sum CF, et al. Metabolic signature shift in type 2 diabetes mellitus revealed by mass spectrometry-based metabolomics. *J Clin Endocrinol Metab* 2013;98:E1060–E1065.
53. O'Brien PD, Guo K, Eid SA, et al. Integrated lipidomic and transcriptomic analyses identify altered nerve triglycerides in mouse models of prediabetes and type 2 diabetes. *Dis Model Mech* 2020;24:13.
54. Huang L, Lin JS, Aris IM, et al. Circulating saturated fatty acids and incident type 2 diabetes: a systematic review and meta-analysis. *Nutrients* 2019;1:11.
55. Tracey TJ, Steyn FJ, Wolvetang EJ, Ngo ST. Neuronal lipid metabolism: multiple pathways driving functional outcomes in health and disease. *Front Mol Neurosci* 2018;11:10.
56. Geraldes P, King GL. Activation of protein kinase C isoforms and its impact on diabetic complications. *Circ Res* 2010;30:1319–1331.
57. Bansal D, Badhan Y, Gudala K, Schifano F. Ruboxistaurin for the treatment of diabetic peripheral neuropathy: a systematic review of randomized clinical trials. *Diabetes Metab J* 2013;37:375–384.
58. Gibellini F, Smith TK. The Kennedy pathway—de novo synthesis of phosphatidylethanolamine and phosphatidylcholine. *IUBMB Life* 2010;62:414–428.
59. Rumora AE, Lentz SI, Hinder LM, et al. Dyslipidemia impairs mitochondrial trafficking and function in sensory neurons. *FASEB J* 2018;32:195–207.
60. Rumora AE, LoGrasso G, Haidar JA, et al. Chain length of saturated fatty acids regulates mitochondrial trafficking and function in sensory neurons. *J Lipid Res* 2019;60:58–70.
61. Rumora AE, LoGrasso G, Hayes JM, et al. The divergent roles of dietary saturated and monounsaturated fatty acids on nerve function in murine models of obesity. *J Neurosci* 2019;8:3770–3781.
62. Hinder LM, Park M, Rumora AE, et al. Comparative RNA-Seq transcriptome analyses reveal distinct metabolic pathways in diabetic nerve and kidney disease. *J Cell Mol Med* 2017;21:2140–2152.
63. Floegel A, Stefan N, Yu Z, et al. Identification of serum metabolites associated with risk of type 2 diabetes using a targeted metabolomic approach. *Diabetes* 2013;62:639–648.
64. Pujol-Lereis LM. Alteration of sphingolipids in biofluids: implications for neurodegenerative diseases. *Int J Mol Sci* 2019;21:20.
65. Yano M, Watanabe K, Yamamoto T, et al. Mitochondrial dysfunction and increased reactive oxygen species impair insulin secretion in sphingomyelin synthase 1-null mice. *J Biol Chem* 2011;4:3992–4002.
66. Martinez-Beamonte R, Lou-Bonafonte JM, Martinez-Gracia MV, Osada J. Sphingomyelin in high-density lipoproteins: structural role and biological function. *Int J Mol Sci* 2013;9:7716–7741.
67. EL Reynolds NR, Akinici G, Henn R, et al., editor. The longitudinal determinants of diabetic complications in the Pima Indians of Arizona. Merrifield, VA: American Diabetes Association; 2020; 80th Virtual Scientific Sessions.
68. Foster DW. Malonyl-CoA: the regulator of fatty acid synthesis and oxidation. *J Clin Invest* 2012;122:1958–1959.

Supporting Information

Additional supporting information may be found online in the Supporting Information section at the end of the article.

File S1. A detailed description about sample preparation, normalization, and metabolite identification performed by Metabolon, Inc.

Table S1. A list of all metabolites identified by Metabolon's global metabolomics analysis. The table includes the mean metabolite levels and a fold change comparison between participant groups for each metabolite.

Figure S1. Boxplots showing the distribution of (A) *p*-values from the linear regression analysis adjusted for age, sex, and medication, (B) *p*-values from the unadjusted *t*-test participant group comparisons, and (C) *Q*-values from the unadjusted *t*-test participant group comparisons.

Figure S2. Boxplots showing the relative abundance of the metabolites that were significantly different between T2D and T2D DPN. Metabolites identified by linear regression included (A) 3-formylindole, (B) tartrate, (C) sulfate of piperine metabolite, (D) 3-carboxy-4-methyl-5-propyl-2-furanpropanoate (CMPF)], (E) 3-bromo-5-chloro-2,6-dihydroxybenzoic acid, (F) N-acetyl-3-methyl-histidine, (G) isoursodeoxycholate sulfate, (H) glycosyl-N-(2-hydroxynervonoyl)-sphingosine (d18:1/24:1(2OH)), (I) citrate, (J) arabinose, (K) 4-methyl-2-oxopentanoate, (L) 3,5-dichloro-2,6-dihydroxybenzoic acid. Metabolites including (M) ximenoylcarnitine (C26:1), (N) perfluorooctanoate, and (O) N-acetyl-β-alanine were identified by elastic net analysis.

Table S2. A list of removed metabolites that were missed in more than 50% of the samples.